Terahertz time-domain spectroscopy and Raman scattering studies of incipient ferroelectric BaZr03

doi: 10.1080/00150193.2016.1173502

Terahertz Time-Domain and Raman Scattering Spectroscopy Studies of $BaZrO_3$

M. A. Helal*, T. Mori, and S. Kojima

Graduate School of Pure and Applied Sciences, University of Tsukuba, Tsukuba, Ibaraki 305-8573, Japan.

E-mail address of the corresponding author: helalphy82@gmail.com

Terahertz Time-Domain and Raman Scattering Spectroscopy Studies of $BaZrO_3$

Abstract: We have studied an incipient ferroelectric $BaZrO_3$ single crystal with perovskite structure by terahertz time-domain and Raman scattering spectroscopies. The phonon-polariton dispersion relation of the low-frequency infrared active TO1 and TO2 modes was studied from the real and imaginary parts of the complex dielectric constants at room temperature. The experimentally observed complex polariton dispersion relations are discussed by a damped harmonic oscillator model. First-order Raman active modes, forbidden in cubic $Pm\bar{3}m$ symmetry, have been observed in a $BaZrO_3$ single crystal, indicating the lowering of cubic symmetry.

Keywords: Perovskite; incipient ferroelectric; THz-TDS; phonon-polariton; Raman scattering.

Introduction

Nowadays, one of the incipient ferroelectric, barium zirconate, $BaZrO_3$ (BZO) with the perovskite structure attracted renewed interest due to its large lattice constant, high melting point, low thermal expansion coefficient, low dielectric loss and low thermal conductivity. According to the X-ray and neutron diffraction studies, BZO was found to be cubic symmetry up to the lowest temperature 2 K and unlike most of the perovskite oxide materials, BZO does not undergo any structural phase transitions [1-3]. Interestingly, a potential structural instability at the *R*-point in the phonon spectrum was observed consistently by the recent first principles calculations [4-6]. As a consequence of the zone- boundary instability, the crystal

is expected to break the symmetry at a sufficiently low temperature and undergo the antiferrodistortive transformation [7]. Very recently, it is reported that the cubic lattice of BZO is slightly distorted due the large ionic radius of a Zr ions (in BZO) than that of the Ti ions (in $BaTiO_3$) causing the change from cubic $Pm\bar{3}m$ to triclinic $P\bar{1}$ symmetry [8]. The $P\bar{1}$ symmetry of BZO was also reported by the first-principles calculations [6].

Recent development of the terahertz time-domain spectroscopy (THz-TDS) has enabled the very promising technique to determine both the real and imaginary parts of the complex dielectric constants of materials in a far-infrared region (IR) accurately. By using the THz pulse reflected or transmitted from a sample, we can directly observe the dielectric property without any assumption or Kramers-Kronig analysis [8,9-11]. Permitivity in the terahertz region, especially, in far-IR, is dominantly determined by the ionic polarization which is derived from the optical phonons. Therefore, it is very important to measure the dielectric spectrum from low frequencies to far-IR because of their contributions of both the dipole and the ionic polarizations to permittivity.

It is well known that the lattice vibrations (polar transverse optical phonons) in a dielectric crystals couple with the electromagnetic waves (photons), and the mixed excitation of phonon and photon is described as a phonon-polariton, resulting in the IR absorption and dielectric abnormality, etc [12-14]. After the discovery of polariton dispersion in a Gallium phosphide, GaP, crystal [15], nowadays, extensive experimental and theoretical research has been carried out in many crystals [16-18]. The recent THz-TDS measurements on a BZO single crystal has been revealed that the lowest-frequency IR active transverse optic (TO) phonon mode near 2 THz exhibit a clear softening upon cooling from 300 to 8 K [8]. Since ferroelectric soft modes propagate as polaritons, therefore, the polariton dispersion in the far-IR gives very important information for both fundamental and technical problems in ferroelectrics. It was confirmed that THz-TDS is a very powerful tool to determine the

polariton dispersion of a ferroelectric soft mode [16]. It is therefore necessary to study the THz dynamics for the characterization of ferroelectric properties. On the basis of the above discussion, in this report, we investigated the complex dispersion relation of phonon-polariton using THz-TDS for an incipient ferroelectric BZO single crystal. In addition, Raman scattering studies have been performed to confirm the symmetry lowering effect in BZO single crystal.

Experiment

Our investigated (001)-oriented BZO single crystal was purchased from the Crystal Base Co. Ltd. with the sizes of 3 × 3 mm^2 and thickness of 0.559 mm. THz transmission spectra were measured by the conventional transmission THz-TDS system (Tochigi Nikon, RT-10,000), where the low temperature grown GaAs photoconductive antennas were used for both the emitter and detector. Femto second pulses with a wavelength of 780 nm were generated by a mode-locked compact fiber laser with a repetition rate of 80 MHz [19-21].

The polarized (VV) and depolarized (VH) Raman scattering spectra at 300 K were measured in the frequency range 20-1000 cm^{-1}. The spectra were excited with the 532 nm line of an Ar laser and recorded in the backward scattering geometry [22] using a double monochromator (Horiba-JY, U-1000) with the additive dispersion.

Results and Discussion

Figure 1 shows the time-domain electric fields of a THz pulse transmitted through a BZO sample as well as through the air reference at 300 K. The THz waveform was delayed due to the attenuation during passing through a BZO sample. In order to determine the complex dielectric constant $\hat{\varepsilon} = \varepsilon' + i\varepsilon''$ from the measured time-domain waveforms, we used the following equation:

$$\frac{E_{sam}(\omega)}{E_{ref}(\omega)} = \frac{4\hat{n}}{(\hat{n}+1)^2} exp\left\{i\frac{(\hat{n}-1)}{c}\omega d\right\} \quad (1)$$

where $\hat{n} = n' + i.n''$ is the complex refractive index, $E_{\text{sam}}(\omega)$ and $E_{\text{ref}}(\omega)$ are the complex amplitude spectra of a THz pulse transmitted through a sample and the reference, respectively, and, c and d are the light velocity and sample thickness, respectively. After then, the complex dielectric constant has been determined from the relation of $\hat{\varepsilon} = \hat{n}^2$. The transmission power spectra of a reference and a BZO single crystal converted from time-domain waveforms at 300 K is shown in Fig. 2 at which a clear absorption mode at about 2.27 THz is observed.

In our previous studies [8], in comparison with the BZO ceramics [23], we concluded that the origin of the newly observed 2 THz mode in a BZO single crystal and an additional mode near 9 THz in BZO ceramics, is due to the lowering of crystal symmetry [8]. It was also pointed out that the lowest frequency TO1 mode in a BZO single crystal is originated from the staggered of oxygen octahedral tilts which have a significant effect on the Last mode. In the present studies, we measured a thin BZO single crystal and it was possible to increase the upper limit of the THz frequency from previously measured 2.7 THz to 3 THz. Therefore, we can more precisely detect the TO2 mode from the slope of ε' and $\varepsilon''$of the complex dielectric constant. Figure 3 (a) shows the ε' and ε'' with open circles at 300 K. In order to determine the mode frequency, dielectric strength, and the damping constant of the TO modes, we have fitted the ε' and ε'' using the following damped harmonic oscillator (DHO) model:

$$\varepsilon(\omega) = \varepsilon(\infty) + \sum_j \frac{\Delta\varepsilon_j \omega_j^2}{\omega_j^2 - \omega^2 - i\omega\Gamma_j} \quad (2)$$

where $\varepsilon(\infty)$ is the high frequency limit of a dielectric constant, and ω_j, $\Delta\varepsilon_j$, and Γ_j are the mode frequency, dielectric strength and damping constant of each oscillator mode, respectively. We assumed two modes for the fitting. The solid lines represent the best fitted line by the DHO model and

the fitting parameters are shown in Table 1. The phonon frequency of the TO2 was obtained at 3.82 THz which is in agreement with recent reflectivity measurements [24] and first-principles calculations [24]. In addition, we have also determined the loss function, Im(1/ ε), from the experimental complex dielectric constant and the results are displayed by open circles along with the calculated one (solid line) by a DHO model in Fig. 3 (b). It is seen from Fig. 3 (b) that almost no LO (longitudinal optic)-TO splitting occurs near 2.27 THz. On the other hand, the LO2 mode appears at around 5.68 THz.

It is well established that in an ionic crystal, the electric fields accompanied with the LO phonons, as irrotational fields, cannot couple with external electric fields. In addition, those accompanied with the TO phonons, as rotational fields, can couple strongly to the electromagnetic waves in the infrared regime and propagates as phonon-polariton. In order to determine the phonon-polariton dispersion relation, we calculated the wave vector of the polariton according to Huang's dispersion relation [13,25]:

$$\varepsilon(k,\omega) = \frac{c^2 k^2(\omega)}{\omega^2} \qquad (3)$$

where ω, k, c, and $\varepsilon(k,\omega)$ are the angular frequency, wave vector, light velocity, and dielectric constant, respectively. In GaP crystal, the polariton dispersion relation was observed for the first time by Raman scattering [15]. However, the damping of the lowest TO mode in GaP was very small and therefore, the polariton dispersion was discussed without considering the polariton damping effect. Moreover, in ferroelectric materials, the damping factor of the soft mode is very large and in some cases the soft mode becomes over damped [26,27]. It is therefore, necessary to discuss the damping effect of the polariton dispersion using a complex dielectric constant.

The dispersion curves of the polaritons were determined from the observed values of the ε' and ε'' of complex dielectric constant up to 3 THz by using Eq. (3). The experimental

results for the imaginary (k'') and real (k') parts of the wave vector at 300 K are shown in Figs. 4 (a) and (b), by the open circles, respectively. The polariton damping in this frequency region is caused by the coupling of the low-frequency soft modes to the electromagnetic part of polariton, respectively. In the case of $LiNbO_3$, the similar type of damping of polaritons was also observed [18,28]. In the BZO, it is already established that the instability around the *R*-points causes the zone-folding effect of phonons at the Γ-points [6,8]. The polariton dispersion relation will be a straight line without the folding effect [18]. Therefore, the phonon-polariton dispersion shows the zone folding effects that result in the interaction with the electromagnetic wave and the folded phonons, and then introduce polaritons with respective order in a tunable frequency regime. The calculated dielectric constants by the DHO model have been used to calculate the polariton dispersion relation with Eq. (3). In Figs. 4 (a) and (b), the calculated polariton dispersion relation at 300 K are presented by the solid lines. The combination of both the experiment and calculation by DHO model shows a very good agreement between theory and experiment.

Figure 5 shows the Raman spectrum of a BZO single crystal measured at 300 K in both the VV and VH scattering geometry. The zone-center optical phonons are of odd parity, and consequently are not Raman active in cubic symmetry [29]. It is seen from Fig. 5 that the spectrum are dominated by the first-order features with broad room temperature maxima. Similar Raman-forbidden first-order peak was also observed in the pure $KTaO_3$ single crystals induced by some unavoidable symmetry breaking defects [30,31]. However, no clear difference has been observed in between VV and VH scattering geometry which reflects the formation of multitwins in a BZO single crystal. The mode frequencies and intensity strength of each mode are presented in Table 2. The appearance of the phonon peaks in the Raman spectrum indicates a lowering of the crystal symmetry in BZO single crystal, induced by the distortion of the oxygen octahedra and thus transforming the crystal symmetry from cubic

$P\mathrm{m}\bar{3}\mathrm{m}$ to triclinic $P\bar{1}$. It is therefore concluded that the origin of the first order Raman scattering in BZO single crystal is caused by the symmetry lowering effect predicted by the recent THz-TDS [8], and first-principles studies [6].

Conclusions

We have investigated the lowest frequency IR active modes of an incipient ferroelectric BZO single crystal by using the broadband THz-TDS in the frequency range between 0.2 to 3 THz. The phonon-polarition dispersion relations were determined from the real and imaginary parts of the complex dielectric constant with high accuracy. The dispersion relations show that the presence of the folding effect in the first Brillouin zone of phonon is responsible for the coupling between photons and phonons, which creates polaritons. The experimentally observed complex polariton dispersion relations were in good agreement within the experimental error with the calculated dispersion curves by the DHO model. The existence of first-order Raman peaks, symmetry forbidden in cubic BZO single crystals, provides a convincing evidence to the symmetry lowering from cubic $P\mathrm{m}\bar{3}\mathrm{m}$ symmetry.

Acknowledgement

This work was supported by the grant in aid from MEXT, Japan.

References

1. Bilic A, and Gale JD: Ground state structure of $BaZrO_3$: A comparative first-principles study. Phys. Rev. B 2009; 79: 174107 (1-9).
2. Zhu C, Xia K, Qian GR, Lu CL, Luo WZ, Wang KF, and Liu J-M: Hydrostatic pressure induced structural instability and dielectric property of cubic $BaZrO_3$. J. Appl. Phys. 2009;105: 044110 (1-8).
3. Akbarzadeh AR, Kornev I, Malibert C, Bellaiche L, and Kiat JM: Combined theoretical and experimental study of the low-temperature properties of $BaZrO_3$. Phys. Rev. B 2005; 72: 205104 (1-8).
4. Zhong W and Vanderbilt D: Competing Structural Instabilities in Cubic Perovskites. Phys. Rev. Lett. 1995; 74: 2587-2590.
5. Levedev AI and Sluchinskaya IA: Structural Instability in $BaZrO_3$ Crystals: Calculations and Experiment. Phys. Solid State 2013; 55: 1941-1945.
6. Bennett JW, Grinberg I, and Rappe AM: Effect of symmetry lowering on the dielectric response of $BaZrO_3$. Phys. Rev. B 2006; 73: 180102 (1-4).
7. Samara GA, Sakudo T, and Yoshimitsu K: Important Generalization Concerning the Role of Competing Forces in Displacive Phase Transitions. Phys. Rev. Lett. 1975; 35: 1767-1769.
8. Helal MA, Mori T, and Kojima S: Softening of infrared-active mode of perovskite $BaZrO_3$ proved by terahertz time-domain spectroscopy. Appl. Phys. Let. 2015; 106: 182904 (1-4).
9. Mori T, Nicol EJ, Shiizuka S, Kuniyasu K, Nojima T, Toyota N, and Carbotte JP: Optical self-energy of superconducting Pb in the terahertz region. Phys. Rev. B 2008; 77: 174515 (1-6).

10. Kojima S, Shibata T, Igawa H, and Mori T: Broadband terahertz time-domain spectroscopy : crystalline and glassy drug materials. IOP conf. series: Mat. Sci. and Eng. 2014; 54: 012001 (1-6).

11. Shibata T, Igawa H, Kim TH, Mori T, and Kojima S: Glass transition dynamics of anti-inflammatory ketoprofen studied by Raman scattering and terahertz time-domain spectroscopy. J. Mol. Struc. 2014; 1062: 185-188.

12. Fano U: Atomic Theory of Electromagnetic Interactions in Dense Materials. Phys. Rev. 1956; 103: 1202-1218.

13. Born M and Huang K: Dynamical theory of crystal lattices, Oxford, 1954.

14. Kittel C: Introduction to solid state physics, 6th ed. (Wiley, New York, 1986).

15. Henry CH and Hopfield JJ: Raman scattering by polaritons. Phys. Rev. Lett. 1965; 15: 964-966.

16. Kojima S, Tsumura N, Takeda MW, and Nishizawa S: Far-infrared phonon-polariton dispersion probed by terahertz time-domain spectroscopy. Phys. Rev. B 2003; 67: 035102 (1-5).

17. Kojima S and Mori T: Broadband terahertz time-domain spectroscopy of ferroelectric $LiTaO_3$: phonon-polariton dispersion. AIP Conf. Proc. 2014; 1627: 52-57.

18. Schwarz UT and Maier M: Damping mechanisms of phonon polaritons, exploited by stimulated Raman gain measurements. Phys. Rev. B 1998; 58, 766-775.

19. Mori T, Igawa H, and Kojima S: Progress of ultrafast terahertz time-domain spectroscopy: Raman inactive soft mode in quantum paraelectric $SrTiO_3$. IOP Conf. Series: Mater. Sci. Eng. 2014; 54: 012006 (1-5).

20. Igawa H, Mori T, and Kojima S: Terahertz time-domain spectroscopy of congruent $LiNbO_3$ and $LiTaO_3$ crystals. Jpn. J. Appl. Phys. 2014; 53: 05FE01 (1-4).

21. Kobayashi Y, Shibata T, Mori T, and Kojima S: Terahertz time-domain spectroscopy and low-frequency Raman scattering of crystalline and glassy pharmaceutical indapamide Int. Lett. Phys. Chem. and Astro. 2015; 46: 16-22.

22. Kojima S: Gigahertz acoustic spectroscopy by micro-Brillouin scattering. Jpn. J. Appl. Phys. 2010;49: 07HA01(1-6).

23. Nuzhnyy D, Petzelt J, Savinov M, Ostapchuk T, Bovtun V, Kempa M, Hlinka J, Buscaglia V, Buscaglia MT, and Nanni P: Broadband dielectric response of $Ba(Zr,Ti)O_3$ ceramics: From incipient via relaxor and diffuse up to classical ferroelectric behaviour. Phy. Rev. B 2012; 86: 014106 (1-9).

24. Evarestov RA: Hybrid density functional theory LCAO calculations on phonons in $Ba(Ti,Zr,Hf)O_3$. Phys. Rev. B 2011; 83: 014105 (1-6).

25. Huang K: On the interaction between radiation field and ionic crystals. Proc. R. Soc. London, Ser. A 1951; 208: 352-356.

26. Laughman L, Davis LW, and Nakamura T: Raman-scattering line shape of the soft E polariton mode in $BaTiO_3$. Phys. Rev. B 1972; 6: 3322-3326.

27. Tominaga Y and Nakamura T: Forward and backward Raman scattering from KH_2PO_4. Ferroelectrics 1978; 21: 317-318.

28. Bittner B, Scherm M, Schoedl T, Tyroller T, Schwarz UT, and Max Maier: Phonon-polariton damping by low-frequency excitations in lithium tantalate investigated by spontaneous and stimulated Raman scattering. J. Phys.: Condens. Matter 2002; 14: 9013-9028.

29. Nilsen WG and Skinner JG: Raman Spectrum of Strontium Titanate. J. Chem. Phys. 1968; 48: 2240-2248.

30. Uwe H, Lyons KB, Carter HL, and Fleury PA: Ferroelectric microregions and Raman scattering in $KTaO_3$. Phys. Rev. B 1986; 33: 6436-6440.

31. Vogt H: J. Phys.: Evidence of defect-induced polarization clusters in nominally pure $KTaO_3$ from low temperature Raman and hyper-Raman spectra. Condens. Matter 1991; 3: 3697-3709.

Table 1. Fitting parameters of Eq. (2) for $BaZrO_3$ at 300 K.

$\boldsymbol{\varepsilon}(\infty)$	$\omega_1(\mathrm{THz})$	$\omega_2(\mathrm{THz})$	$\Delta\varepsilon_1$	$\Delta\varepsilon_2$	$\Gamma_1(\mathrm{THz})$	$\Gamma_2(\mathrm{THz})$
16	2.27	3.82	0.26	19.67	0.42	0.08

Table 2. Phonon mode frequencies and intensity strength of $BaZrO_3$ at 300 K by Raman scattering.

Mode frequency (cm^{-1})	Intensity strength
194	Weak
292	Strong
352	Medium
422	Medium
487	Weak
593	Weak
600	Strong
637	Weak
696	Weak
741	Medium
832	Weak

Figure Captions

Fig. 1. Time-domain waveforms of the reference (solid black line) and BZO sample (solid red line) at 300 K.

Fig. 2. The power spectra of the reference (solid blue line) and BZO sample (solid orange line) at 300 K.

Fig. 3. (a) The real and imaginary parts of the complex dielectric constant of BZO at 300 K. The experimental and fitting results are shown by open circles and solid lines, respectively. (b) The loss function of BZO at 300 K are shown by open circles. The solid line represents the calculated one by DHO model.

Fig. 4. Polariton dispersion relation of (a) the imaginary and (b) real parts of the wave vector. The open circles have been measured at 300 K using THz-TDS. The solid curves have been calculated using the DHO model.

Fig. 5. Raman scattering spectrum of a BZO single crystal at 300 K.

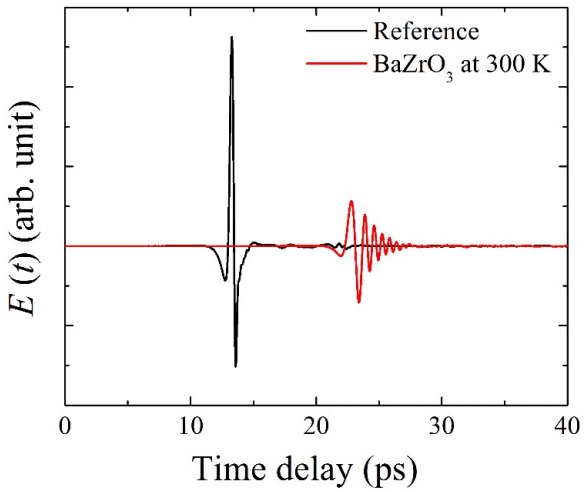

Figure 1.

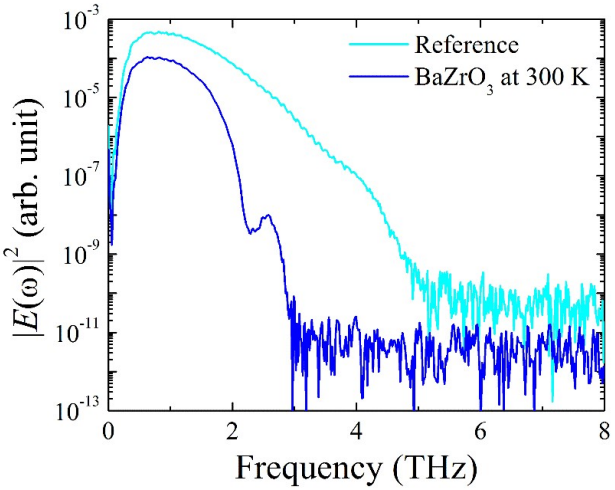

Figure 2.

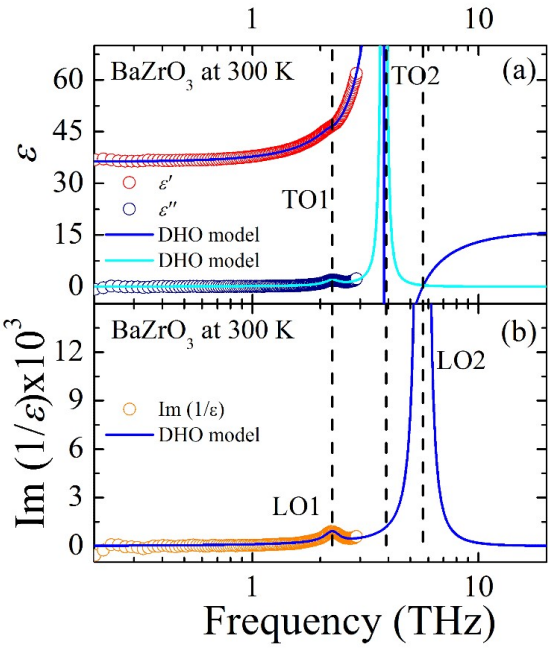

Figure 3.

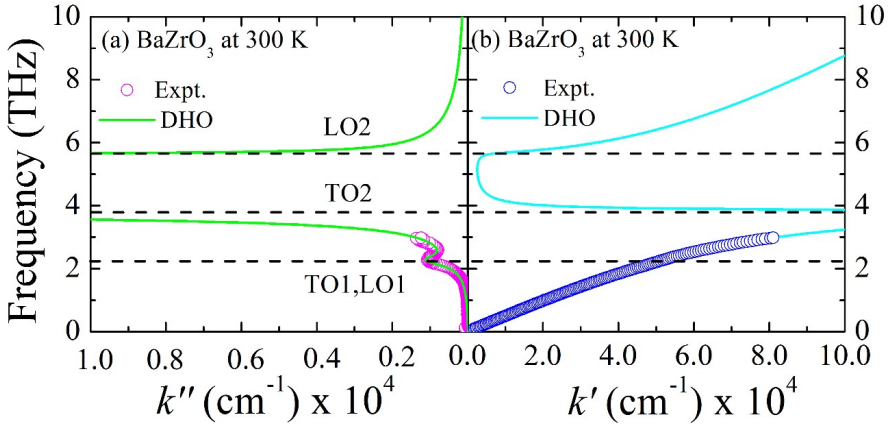

Figure 4.

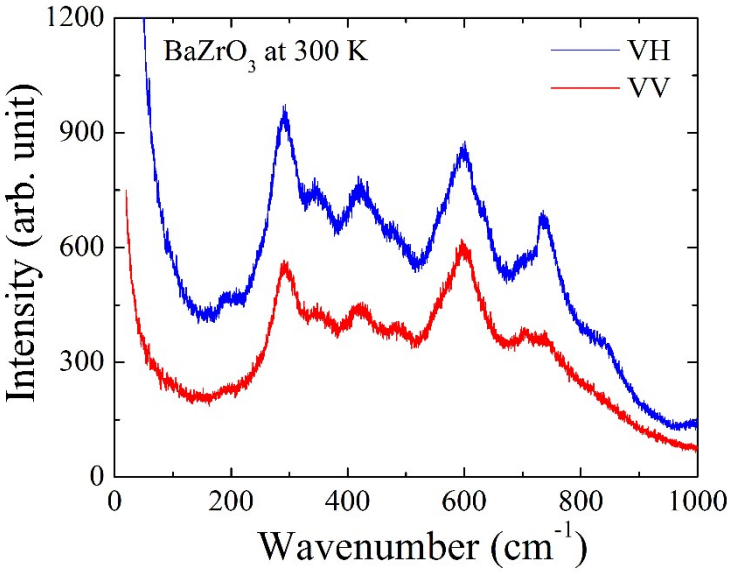
BaZrO3 at 300 K
VH
VV
Intensity (arb. unit)
Wavenumber (cm-1)
0
300
600
900
1200
0
200
400
600
800
1000

Figure 5.